JOURNAL OF SPACECRAFT AND ROCKETS
Vol. 42, No. 6, November–December 2005

Engineering Notes

ENGINEERING NOTES are short manuscripts describing new developments or important results of a preliminary nature. These Notes should not exceed 2500 words (where a figure or table counts as 200 words). Following informal review by the Editors, they may be published within a few months of the date of receipt. Style requirements are the same as for regular contributions (see inside back cover).

Optimal Control Laws for Axially Symmetric Solar Sails

Giovanni Mengali* and Alessandro A. Quarta†
University of Pisa, I-56122 Pisa, Italy

Introduction

THE performance of a solar sail spacecraft is remarkably affected by the geometry and the sail film optical properties.[1] A comparison between various models is extremely useful for mission analysis purposes, and significant results can be established through the study of optimal interplanetary trajectories. A comprehensive discussion of this subject for ideal and nonideal flat sails is reported in Refs. 2 and 3. However, realistic sail models should include the nonplanar sail shape and/or the billowing effect due to the solar radiation pressure. Currently, the only results available for three-dimensional geometries are the optimal steering laws for the so-called parametric-force model.[3,4] Nevertheless, this model is specific for a certain class of solar sails in that it has been established through a best fit of experimental data obtained with Jet Propulsion Laboratory sails.[4]

Recently, Rios-Reyes and Scheeres have characterized a generic three-dimensional sail geometry through a fixed number of numerical coefficients.[5] However, the determination of the optimal control law for a generic sail shape still remains a formidable task because the sail acceleration is a function of two independent control variables: the cone angle (which defines the direction of the incoming radiation with respect to a sail-fixed axis z) and the clock angle (which defines the sunlight direction measured on a plane orthogonal to z).

The aim of this Note is to show that the problem of optimal trajectories is analytically tractable for three-dimensional sail geometries provided that the sail surface presents some symmetries. In particular, this is true for axially symmetric solar sails, which are studied hereafter. Assuming a sail fixed direction coincident with the symmetry axis, the sailcraft acceleration is independent of the clock angle, and the optimal steering law for minimum-time trajectories is found using an indirect approach. This result is shown to include the flat sail model as a particular case.

Equations of Motion

The equations of motion for a sailcraft in a heliocentric inertial frame are

$$\dot{\boldsymbol{r}} = \boldsymbol{v} \tag{1}$$

$$\dot{\boldsymbol{v}} = -(\mu_\odot / r^3)\boldsymbol{r} + \boldsymbol{a} \tag{2}$$

where $\boldsymbol{r}$ and $\boldsymbol{v}$ are the sailcraft position and velocity, whereas $\boldsymbol{a}$ is the acceleration due to the solar radiation pressure. The acceleration experienced by a sailcraft of arbitrary sail geometry can be characterized with the aid of the model proposed by Rios-Reyes and Scheeres.[5] To this end, let s be the fraction of photons specularly reflected by the sail, B_f and B_b the non-Lambertian coefficients of the front and back sail surfaces, ϵ_f and ϵ_b the corresponding front and back emissivities, and $\rho < 1$ be the reflection coefficient. Assume that the sail does not change shape as its attitude varies and that there is no self-shadowing effect. When the position unit vector $\hat{\boldsymbol{r}}$ and the normal unit vector at any point on the sail $\hat{\boldsymbol{n}}$ are introduced, the propulsive acceleration takes the form[5]

$$\boldsymbol{a} = (P/m)\left[a_2 \boldsymbol{J}^{(2)} \cdot \hat{\boldsymbol{r}} - (a_1 - a_3)\hat{\boldsymbol{r}} \cdot \boldsymbol{J}^{(3)} \cdot \hat{\boldsymbol{r}} - a_3 \left(\boldsymbol{J}^{(1)} \cdot \hat{\boldsymbol{r}}\right)\hat{\boldsymbol{r}}\right] \tag{3}$$

where $P = P(r)$ is the solar radiation pressure, m is the spacecraft mass, $\boldsymbol{J}^{(k)}$, $k = 1, 2, 3$, is a rank-k tensor computed by integrating the outer product of the normal unit vectors $\hat{\boldsymbol{n}}$ over the reflecting surface area A of the sail, that is,

$$\boldsymbol{J}^{(k)} \triangleq \int_A \hat{\boldsymbol{n}}^k \, \mathrm{d}A \tag{4}$$

and the force coefficients a_1, a_2, and a_3 are defined as

$$a_1 \triangleq 1 + \rho s; \qquad a_2 \triangleq B_f \rho (1 - s) + (1 - \rho)\frac{\epsilon_f B_f - \epsilon_b B_b}{\epsilon_f + \epsilon_b}$$

$$a_3 \triangleq 1 - \rho s \tag{5}$$

When constant force coefficients are assumed, for a given sail shape the tensors $\boldsymbol{J}^{(1)}$, $\boldsymbol{J}^{(2)}$, and $\boldsymbol{J}^{(3)}$ need be computed just once in a sail-fixed reference frame and are independent of the solar incident direction $\hat{\boldsymbol{r}}$. Also, by definition,[6] $\boldsymbol{J}^{(2)}$ and $\boldsymbol{J}^{(3)}$ are completely symmetric tensors. It is known that a rank-3 completely symmetric tensor is characterized by 10 distinct terms.[6] Accordingly, the propelling acceleration experienced by a solar sail depends on 19 scalar quantities: 3 associated to $\boldsymbol{J}^{(1)}$, 6 to $\boldsymbol{J}^{(2)}$, and 10 to $\boldsymbol{J}^{(3)}$. This result corrects a minor error in Ref. 5.

Let $\mathcal{T}(x, y, z)$ be a sail-fixed reference frame whose unit vectors are $\hat{\boldsymbol{i}}$, $\hat{\boldsymbol{j}}$, and $\hat{\boldsymbol{k}}$. For a generic sail geometry, Eq. (3) states that the sail acceleration is a function of the cone angle α, the angle between $\hat{\boldsymbol{k}}$ and $-\hat{\boldsymbol{r}}$, and of the clock angle δ, the angle between $\hat{\boldsymbol{i}}$ and the projection of $\hat{\boldsymbol{r}}$ on the plane (x, y). In other terms, at any time instant both α and δ must be specified to define fully the sail steering law. The dependence of the thrust vector on two independent control variables, α and δ, is highly undesirable due the difficulties that arise in a practical implementation of a complex sailcraft control law. In particular, it is highly desirable to eliminate the explicit dependence of the steering law on the clock angle, which is difficult to measure. A possible solution to the problem is choosing an axially symmetric configuration in which, as is shown later, the thrust vector lies in the plane defined by the position vector and the symmetry axis.

Axially Symmetric Sail

Equation (3) is remarkably simplified when the sail has axial symmetry. Consider again the earlier defined sail-fixed frame $\mathcal{T}$ and let z coincide with the symmetry axis. Assume that the whole sail surface belongs to the half-space $z \geq 0$. Let $\boldsymbol{r}_s$ be the vector position

Received 11 April 2005; revision received 10 June 2005; accepted for publication 13 June 2005.

*Associate Professor, Department of Aerospace Engineering; g.mengali@ing.unipi.it.

†Research Assistant, Department of Aerospace Engineering; a.quarta@ing.unipi.it.

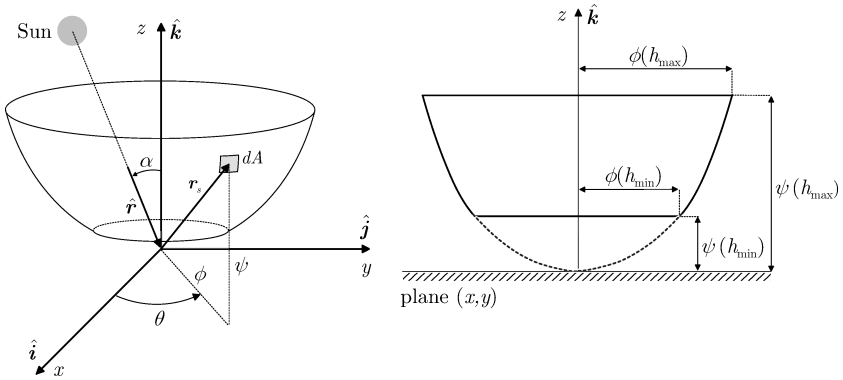

Fig. 1 Solar sail geometry and sail-fixed reference frame.

from the frame origin to the center of a differential surface dA of the sail. When the standard parameterization of a surface of revolution[7] is used, (with independent variables h and θ), the components of $\boldsymbol{r}_s$ in the $\mathcal{T}$ frame can be formally expressed as

$$[\boldsymbol{r}_s]_{\mathcal{T}} = [\phi\cos\theta, \phi\sin\theta, \psi]^T \tag{6}$$

where $\phi = \phi(h) > 0$, $\psi = \psi(h) \geq 0$, $h \in [h_{\min}, h_{\max}]$, and $\theta \in [0, 2\pi]$ (Fig. 1).

The unit vector $\hat{\boldsymbol{n}}$ normal to the differential surface dA is given by

$$[\hat{\boldsymbol{n}}]_{\mathcal{T}} = \left(1\Big/\sqrt{\phi'^2 + \psi'^2}\right)[-\psi'\cos\theta, -\psi'\sin\theta, \phi']^T \tag{7}$$

where the prime ($'$) means differentiation with respect to the variable h. Finally, dA can be expressed as a function of h and θ as

$$\mathrm{d}A = \phi\sqrt{\phi'^2 + \psi'^2}\,\mathrm{d}h\,\mathrm{d}\theta \tag{8}$$

Substituting Eqs. (7) and (8) into Eq. (4) and retaining only the nonzero components of $\boldsymbol{J}^{(k)}$ gives the following expression for the sailcraft acceleration:

$$\boldsymbol{a} = (P/m)(f_r\hat{\boldsymbol{r}} - f_z\hat{\boldsymbol{k}}) \tag{9}$$

where

$$f_r \triangleq a_2 J_{11}^{(2)} + \left[2(a_1 - a_3)J_{223}^{(3)} + a_3 J_3^{(1)}\right]\cos\alpha \tag{10}$$

$$f_z \triangleq (a_1 - a_3)J_{223}^{(3)} + a_2\left(J_{33}^{(2)} - J_{11}^{(2)}\right)\cos\alpha + (a_1 - a_3)\left(J_{333}^{(3)} - 3J_{223}^{(3)}\right)\cos^2\alpha \tag{11}$$

In Eqs. (10) and (11), the sail cone angle $\alpha \in [0, \alpha_{\max}]$ is defined as (Fig. 1)

$$\cos\alpha \triangleq -\hat{\boldsymbol{r}}\cdot\hat{\boldsymbol{k}} \tag{12}$$

and $\alpha_{\max} \leq \pi/2$ is the value of α beyond which the assumption of no self-shadowing effect fails. When a convex surface is assumed, $\alpha_{\max}$ is related to the maximum value of $\phi'(h)$ in the range $[h_{\min}, h_{\max}]$ as

$$\tan\alpha_{\max} = \max(\phi'/\psi') \tag{13}$$

As is clear from Eqs. (10) and (11), the tensors $\boldsymbol{J}^{(1)}$, $\boldsymbol{J}^{(2)}$, and $\boldsymbol{J}^{(3)}$ now depend on only five scalar quantities. When Eqs. (4), (7), and (8) are used, their components can be expressed as a function of ϕ and ψ as follows:

$$J_3^{(1)} = 2\pi\int_{h_{\min}}^{h_{\max}} \phi'\phi\,\mathrm{d}h = A_p \tag{14}$$

$$J_{11}^{(2)} = \pi\int_{h_{\min}}^{h_{\max}} \frac{\psi'^2\phi}{\sqrt{\phi'^2 + \psi'^2}}\,\mathrm{d}h \tag{15}$$

$$J_{33}^{(2)} = 2\pi\int_{h_{\min}}^{h_{\max}} \frac{\phi'^2\phi}{\sqrt{\phi'^2 + \psi'^2}}\,\mathrm{d}h \tag{16}$$

$$J_{223}^{(3)} = \pi\int_{h_{\min}}^{h_{\max}} \frac{\psi'^2\phi\phi'}{\phi'^2 + \psi'^2}\,\mathrm{d}h \tag{17}$$

$$J_{333}^{(3)} = 2\pi\int_{h_{\min}}^{h_{\max}} \frac{\phi'^3\phi}{\phi'^2 + \psi'^2}\,\mathrm{d}h \tag{18}$$

where $A_p \triangleq \pi[\phi^2(h_{\max}) - \phi^2(h_{\min})]$ is the reflecting surface projected on the plane (x, y). Equation (9) implies that the sail acceleration belongs to the plane $(\hat{\boldsymbol{r}}, \hat{\boldsymbol{k}})$, which, by definition, is a symmetry plane for the sail. This is a fundamental result in that the sail acceleration does not depend on the clock angle δ.

More generally, it can be shown that Eq. (9) holds true for a generic sail having a symmetry plane, provided that the unit vector $\hat{\boldsymbol{r}}$ belongs to this plane. From a practical standpoint, a configuration with a symmetry plane does not simplify the optimal steering law because small sail rotations around $\hat{\boldsymbol{r}}$ would cause unwanted accelerations out of the symmetry plane and, in consequence, would make the thrust vector depend on the clock angle δ.

It is interesting to specialize Eqs. (14–18) in the limiting case of a planar surface. This situation is characterized by $\psi(h) = \text{const}$, or $\psi' \equiv 0$. Accordingly, it is easily checked that Eqs. (14–18) reduce to

$$J_3^{(1)} = J_{33}^{(2)} = J_{333}^{(3)} = A_p; \qquad J_{11}^{(2)} = J_{223}^{(3)} = 0 \tag{19}$$

As a result, Eq. (9) boils down to the expression of the acceleration experienced by a flat sail with an optical force model.[3] Thus, Eq. (9) represents an extension to a three-dimensional case of the force model valid for a flat sail.

Optimal Control Law

We now address the optimal control law $\boldsymbol{u}(t) = [\alpha(t), \delta(t)]^T$ that minimizes the time t_f necessary to transfer the spacecraft from an initial $(\boldsymbol{r}_0, \boldsymbol{v}_0)$ to a final $(\boldsymbol{r}_f, \boldsymbol{v}_f)$ prescribed state. This amounts to maximizing the performance index:

$$J = -t_f \tag{20}$$

From Eqs. (1) and (2), the Hamiltonian of the system is

$$H = \boldsymbol{\lambda}_r\cdot\boldsymbol{v} - (\mu_\odot/r^3)\boldsymbol{\lambda}_v\cdot\boldsymbol{r} + H' \tag{21}$$

where $H' \triangleq \boldsymbol{\lambda}_v\cdot\boldsymbol{a}$ is that portion of the Hamiltonian that explicitly depends on the control vector. Also, $\boldsymbol{\lambda}_r$ is the vector adjoint to the position, and $\boldsymbol{\lambda}_v$ is the primer vector. Invoking Pontryagin's maximum principle, the optimal control law is such that, at any time, H' is an absolute maximum. From Eq. (21), the optimal control law is obtained by looking for the direction of $\hat{\boldsymbol{k}}$ that maximizes, at any time, the projection of the propelling acceleration $\boldsymbol{a}$ on the direction of the primer vector $\hat{\boldsymbol{\lambda}}_v \triangleq \boldsymbol{\lambda}_v/\|\boldsymbol{\lambda}_v\|$.

When an approach similar to that outlined in Ref. 3 is used, it can be verified that the optimal steering law does not depend on the clock angle δ and that the vectors $\hat{\boldsymbol{k}}$, $\hat{\boldsymbol{r}}$, and $\hat{\boldsymbol{\lambda}}_v$ are coplanar. Let α_λ

denote the primer vector cone angle, that is, the angle between $\hat{\boldsymbol{r}}$ and $\hat{\boldsymbol{\lambda}}_v$, and consider the function f defined as

$$\alpha_\lambda = f(\alpha): \qquad \frac{\partial H'}{\partial \alpha}(\alpha, f(\alpha)) = 0 \tag{22}$$

In other terms, for a given α, $f(\alpha)$ is the value of α_λ that renders the Hamiltonian stationary. Setting $\partial H'/\partial\alpha = 0$ yields

$$\alpha_\lambda = f(\alpha) = \tan^{-1}\frac{\sin\alpha\,(\mathcal{A}\cos^2\alpha + 2\mathcal{B}\cos\alpha + \mathcal{C})}{\mathcal{A}\cos^3\alpha + 2\mathcal{B}\cos^2\alpha + \mathcal{D}\cos\alpha - \mathcal{B}} \tag{23}$$

where

$$\mathcal{A} \triangleq 3(a_1 - a_3)\left(3J^{(3)}_{223} - J^{(3)}_{333}\right) \tag{24}$$

$$\mathcal{B} \triangleq a_2\left(J^{(2)}_{11} - J^{(2)}_{33}\right) \tag{25}$$

$$\mathcal{C} \triangleq 3(a_3 - a_1)J^{(3)}_{223} - a_3 J^{(1)}_3 \tag{26}$$

$$\mathcal{D} \triangleq (a_1 - a_3)\left(2J^{(3)}_{333} - 7J^{(3)}_{223}\right) \tag{27}$$

Also, let α^* be the point such that

$$\alpha^* = \max_{0\le\alpha\le\alpha_{\max}} \alpha: \qquad H'(\alpha, f(\alpha)) \ge H'(\alpha_{\max}, f(\alpha)) \tag{28}$$

and define

$$\alpha^*_\lambda \triangleq f(\alpha^*) \tag{29}$$

Then, the optimal control law is

$$\alpha = \begin{cases} f^{-1}(\alpha_\lambda), & \text{if} \quad \alpha_\lambda \in \left[0, \alpha^*_\lambda\right) \\ \alpha_{\max}, & \text{if} \quad \alpha_\lambda \in \left[\alpha^*_\lambda, \pi\right] \end{cases} \tag{30}$$

where $\alpha = f^{-1}(\alpha_\lambda)$ is the solution of Eq. (23) with respect to α.

Although an explicit solution for $\alpha = f^{-1}(\alpha_\lambda)$ cannot be obtained from Eq. (23), note that $f(\alpha)$ is only a function of the sail optical properties and geometry. Accordingly, it is possible to calculate numerically a set of pairs $(\alpha_i, \alpha_{\lambda_i})$ from Eq. (23) and interpolate $f^{-1}(\alpha_\lambda)$ over the interval $[0, \alpha_{\max}]$.

It is interesting to investigate the special case of flat sail. When Eqs. (19) are substituted into Eqs. (24–27), Eq. (23) reduces to

$$\tan\alpha_\lambda = \frac{\sin\alpha\left[3(a_1 - a_3)\cos^2\alpha + 2a_2\cos\alpha + a_3\right]}{3(a_1 - a_3)\cos^3\alpha + 2a_2\cos^2\alpha - 2(a_1 - a_3)\cos\alpha - a_2} \tag{31}$$

and coincides with the result found in Ref. 3 for a flat sail with optical force model. It can also be verified that $\alpha_{\max} = \pi/2$ and that α^*_λ corresponds to the critical cone angle defined in Ref. 3.

Examples of Geometrical Configurations

We now specialize Eqs. (14–18) to some representative geometrical configurations. In the following examples, the sail geometry is that of Fig. 1.

Frustum of a Cone

Consider a frustum of a cone and let ζ be the half-opening angle of the cone. The parameterization of the conical surface is

$$\psi = h, \qquad \phi = h\tan\zeta \tag{32}$$

From Eqs. (14–18), the components of $\boldsymbol{J}^{(1)}$, $\boldsymbol{J}^{(2)}$, and $\boldsymbol{J}^{(3)}$ defining the sail propelling acceleration are

$$J^{(1)}_3 = \pi\tan^2\zeta\left(h^2_{\max} - h^2_{\min}\right) = A_p, \qquad J^{(2)}_{11} = \frac{J^{(1)}_3\cos^2\zeta}{2\sin\zeta}$$

$$J^{(2)}_{33} = J^{(1)}_3\sin\zeta \tag{33}$$

$$J^{(3)}_{223} = \frac{1}{2}J^{(1)}_3\cos^2\zeta, \qquad J^{(3)}_{333} = J^{(1)}_3\sin^2\zeta \tag{34}$$

In particular, for a given value of A_p and assuming $\zeta = \pi/2$, the problem reduces to a flat sail and, as expected, Eqs. (33) and (34) coincide with Eq. (19).

Frustum of a Paraboloid

Consider a sail whose shape is a frustum of a paraboloid. The parametric equations are

$$\psi = h, \qquad \phi = \sqrt{2hp} \tag{35}$$

where p is the semilatus rectum of the parabola obtained through the intersection between the surface of revolution and a meridian plane.

The components of $\boldsymbol{J}^{(1)}$, $\boldsymbol{J}^{(2)}$, and $\boldsymbol{J}^{(3)}$ defining the propelling acceleration are

$$J^{(1)}_3 = 2\pi p(h_{\max} - h_{\min}) = A_p \tag{36}$$

$$J^{(2)}_{11} = -\frac{2}{3}\sqrt{p}\pi\left[\sqrt{p + 2h_{\max}}(p - h_{\max}) - \sqrt{p + 2h_{\min}}(p - h_{\min})\right] \tag{37}$$

$$J^{(2)}_{33} = 2p\sqrt{p}\pi\left(\sqrt{p + 2h_{\max}} - \sqrt{p + 2h_{\min}}\right) \tag{38}$$

$$J^{(3)}_{223} = \frac{1}{2}p\pi\left[2(h_{\max} - h_{\min}) + p\log\left(\frac{p + 2h_{\min}}{p + 2h_{\max}}\right)\right] \tag{39}$$

$$J^{(3)}_{333} = \pi p^2\log\left(\frac{p + 2h_{\max}}{p + 2h_{\min}}\right) \tag{40}$$

The planar case is recovered in the limit as $h_{\max}/p$ tends to zero.

Spherical Zone

Consider a spherical zone of given radius R. The parametric equations are

$$\psi = h; \qquad \phi = \sqrt{h(2R - h)} \tag{41}$$

The components of $\boldsymbol{J}^{(1)}$, $\boldsymbol{J}^{(2)}$, and $\boldsymbol{J}^{(3)}$ defining the propelling acceleration are

$$J^{(1)}_3 = \pi(h_{\min} - h_{\max})(h_{\min} + h_{\max} - 2R) = A_p \tag{42}$$

$$J^{(2)}_{11} = \frac{J^{(1)}_3}{3}\frac{h^2_{\min} - 3Rh_{\min} + h_{\min}h_{\max} - 3Rh_{\max} + h^2_{\max}}{R(h_{\min} + h_{\max} - 2R)} \tag{43}$$

$$J^{(2)}_{33} = -\frac{2J^{(1)}_3}{3}\frac{h^2_{\min} - 3Rh_{\min} + h_{\min}h_{\max} - 3Rh_{\max} + h^2_{\max} + 3R^2}{R(h_{\min} + h_{\max} - 2R)} \tag{44}$$

$$J^{(3)}_{223} = J^{(1)}_3\frac{2Rh_{\min} + 2Rh_{\max} - h^2_{\min} - h^2_{\max}}{4R^2} \tag{45}$$

$$J^{(3)}_{333} = -J^{(1)}_3\frac{2Rh_{\min} + 2Rh_{\max} - h^2_{\min} - h^2_{\max} - 2R^2}{2R^2} \tag{46}$$

These coefficients agree with Rios-Reyes and Scheeres.[5] The planar case is approached in the limit where $h_{\max}/R$ tends to zero.

Numerical Example

For illustrative purposes, conical sails with different half-opening angles of the cone have been compared in terms of minimum-time Earth–Mars orbit transfers. Circular and coplanar planetary orbits are assumed. A set of canonical units have been used in the integration of the differential equations to reduce their numerical sensitivity. The differential equations have been integrated in double precision using a Runge–Kutta fifth-order scheme with absolute and relative errors of 10^{-10}. The boundary-value problem associated to the variational problem has been solved through a hybrid numerical technique combining genetic algorithms (to obtain an estimate of the

adjoint variables) with gradient-based and direct methods to refine the solution.[3]

Figure 2 shows the critical cone angle α^* [see Eq. (28)] as a function of the half-opening angle ζ. Note that for a conical sail $\zeta \equiv \alpha_{\max}$ [see Eq. (13)]. Basically, α^* comes from two distinct constraints: the requirement of no self-shadowing effect and the maximization of the Hamiltonian. More precisely, recall Eq. (22), define $\bar{\alpha}_\lambda \triangleq \max f(\alpha)$, and let $\bar{\alpha} = f^{-1}(\bar{\alpha}_\lambda)$. The linear behavior between

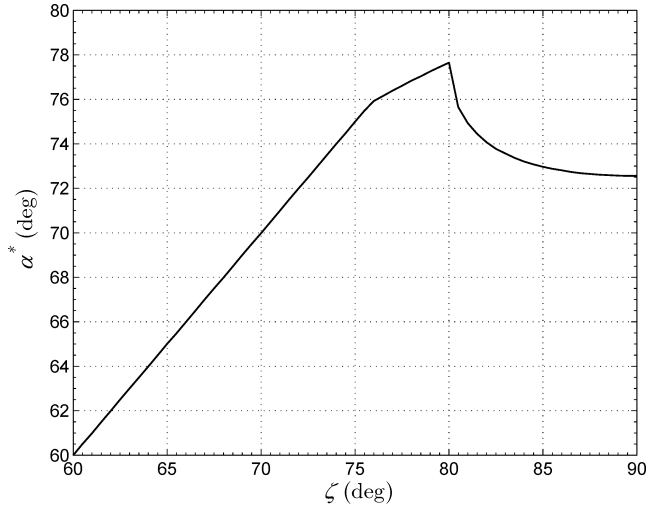

Fig. 2 Critical cone angle α^* for conical sail.

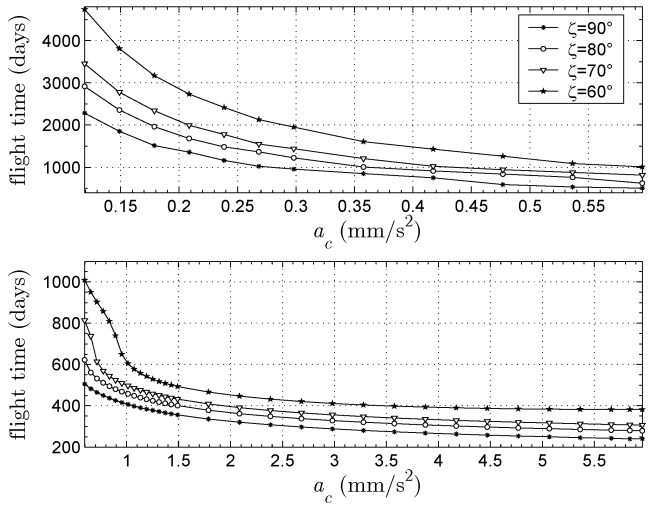

Fig. 3 Mission times for a Earth–Mars circle-to-circle transfer with conical solar sail.

α^* and ζ in Fig. 2 corresponds to a situation in which $\bar{\alpha} > \alpha_{\max}$ and $H'(\bar{\alpha}, \bar{\alpha}_\lambda) > 0$. In this case, the value of α^* results from avoiding self-shadowing effects. For $\zeta \in [76\text{ deg}, 80\text{ deg}]$, it happens that $\bar{\alpha} < \alpha_{\max}$ and $H'(\bar{\alpha}, \bar{\alpha}_\lambda) > 0$. Finally, when $\zeta > 80$ deg, one has $\bar{\alpha} < \alpha_{\max}$ and $H'(\bar{\alpha}, \bar{\alpha}_\lambda) < 0$. In the latter case, the Hamiltonian value decreases as α increases and a turning point appears in Fig. 2. In the limiting case as ζ approaches 90 deg, a flat sail model is recovered, and the corresponding variation of the Hamiltonian with α is shown in Ref. 3.

Finally, Fig. 3 shows the mission times as a function of the solar sail characteristic acceleration[4] a_c, calculated using the surface A_p [see Eq. (14)]. The case $\zeta = 90$ deg corresponds to a flat sail. As expected, the mission times are affected by ζ, with a remarkable performance degradation for low values of the characteristic acceleration. For instance, when $a_c = 1$ mm/s^2 is assumed, the percentage increment in mission times with respect to a flat sail are on the order of 13, 22, and 50% for $\zeta = 80$, 70, and 60 deg, respectively.

Conclusions

A generic model of an axially symmetric solar sail has been investigated. The acceleration experienced by the sail is shown to depend on five scalar quantities and to belong to the plane containing the direction of the incoming radiation and the sail symmetry axis. The optimal control law for minimum-time interplanetary trajectories has been found using an indirect approach. The steering law is found to be independent of the clock angle and to extend the results for a flat sail to a three-dimensional axially symmetric geometry.

References

[1]Dachwald, B., "Minimum Transfer Times for Nonperfectly Reflecting Solar Sailcraft," *Journal of Spacecraft and Rockets*, Vol. 41, No. 4, 2004, pp. 693–695.

[2]Sauer, C. G., Jr., "Optimum Solar-Sail Interplanetary Trajectories," AIAA Paper 76-0792, Aug. 1976.

[3]Mengali, G., and Quarta, A. A., "Optimal Three-Dimensional Interplanetary Rendezvous Using Nonideal Solar Sail," *Journal of Guidance, Control, and Dynamics*, Vol. 28, No. 1, 2005, pp. 173–177.

[4]Wright, J. L., *Space Sailing*, Gordon and Breach Science, Philadelphia, 1992, pp. 2, 227–233.

[5]Rios-Reyes, L., and Scheeres, D. J., "Generalized Models for Solar Sails," *Journal of Spacecraft and Rockets*, Vol. 42, No. 1, 2005, pp. 182–185.

[6]Sokolnikoff, I. S., *Tensor Analysis, Theory and Applications*, Wiley, New York, 1958, pp. 100–104.

[7]Gray, A., *Modern Differential Geometry of Curves and Surfaces with Mathematica*, 2nd ed., CRC Press, Boca Raton, FL, 1997, Chap. 20, pp. 457–480.

D. Spencer
Associate Editor